Available online at www.sciencedirect.com
ScienceDirect
Biochimica et Biophysica Acta 1767 (2007) 712–724
Biochimica et Biophysica Acta BBA
www.elsevier.com/locate/bbabio

Chemical rescue of a site-modified ligand to a [4Fe–4S] cluster in PsaC, a bacterial-like dicluster ferredoxin bound to Photosystem I

Mikhail L. Antonkine [a,d,e,*,1], Estelle M. Maes [b], Roman S. Czernuszewicz [b], Christoph Breitenstein [e], Eckhard Bill [e], Christopher J. Falzone [c], Ramakrishnan Balasubramanian [a], Carolyn Lubner [c], Donald A. Bryant [a], John H. Golbeck [a,c]

[a] *Department of Biochemistry and Molecular Biology, The Pennsylvania State University, University Park, PA 16802, USA*
[b] *Department of Chemistry, University of Houston, Houston, TX 77204, USA*
[c] *Department of Chemistry, The Pennsylvania State University, University Park, PA 16802, USA*
[d] *Institut für Experimentalphysik, Freie Universität Berlin, Arnimallee 14, D-14195 Berlin, Germany*
[e] *Max-Planck-Institut für Bioanorganische Chemie, Stifistr. 34-36, Mülheim an der Ruhr, D-45470, Germany*

Received 28 September 2006; received in revised form 21 January 2007; accepted 2 February 2007
Available online 9 February 2007

Abstract

Chemical rescue of site-modified amino acids using externally supplied organic molecules represents a powerful method to investigate structure–function relationships in proteins. Here we provide definitive evidence that aryl and alkyl thiolates, reagents typically used for *in vitro* iron–sulfur cluster reconstitutions, serve as rescue ligands to a site-specifically modified $[4Fe–4S]^{1+,2+}$ cluster in PsaC, a bacterial dicluster ferredoxin-like subunit of Photosystem I. PsaC binds two low-potential $[4Fe–4S]^{1+,2+}$ clusters termed F_A and F_B. In the C13G/C33S variant of PsaC, glycine has replaced cysteine at position 13 creating a protein that is missing one of the ligating amino acids to iron–sulfur cluster F_B. Using a variety of analytical techniques, including non-heme iron and acid-labile sulfur assays, and EPR, resonance Raman, and Mössbauer spectroscopies, we showed that the C13G/C33S variant of PsaC binds two $[4Fe–4S]^{1+,2+}$ clusters, despite the absence of one of the biological ligands. ^{19}F NMR spectroscopy indicated that the external thiolate replaces cysteine 13 as a substitute ligand to the F_B cluster. The finding that site-modified $[4Fe–4S]^{1+,2+}$ clusters can be chemically rescued with external thiolates opens new opportunities for modulating their properties in proteins. In particular, it provides a mechanism to attach an additional electron transfer cofactor to the protein *via* a bound, external ligand.

Keywords: Photosystem I; PsaC; $S \geq 3/2$; [4Fe–4S] cluster; Iron–sulfur protein; Chemical rescue

1. Introduction

Since the pioneering work of Toney and Kirsch, in which the activity of a Lys658Ala variant of aspartate aminotransferase was restored by the addition of primary amines [1], chemical rescue of site-modified amino acids with externally supplied organic molecules has developed into a powerful method to explore structure–function relationships in proteins. The majority of such studies have involved changing basic Arg, His or Lys residues to Ala and rescuing of enzymatic activity with imidazole [2–9] or primary amines [1,10–14]; changing acidic Asp or Glu residues to neutral amino acids (Ala, Gly, Ser) and rescuing enzyme activity with azide [15–20] or acetate [21,22]; or changing Tyr residues to Thr or Gly and rescuing enzyme activity with phenols [23,24]. Additional strategies have included altering Arg or Lys residues to Cys, which could be rescued by chemical modification (e.g., aminoethylation) to restore activity [25–27], and altering carbamylated Lys residues to Glu followed by rescue of activity with organic acids such as formate [28,29]. In many of these studies, the role of a particular

Abbreviations: PS I, Photosystem I; EPR, electron paramagnetic resonance; NMR, nuclear magnetic resonance; F_A and F_B, the two [4Fe–4S] clusters of PsaC; P700-F_X core, a PS I preparation in which the stromal polypeptides PsaC, PsaD and PsaE, together with [4Fe–4S] clusters F_A and F_B, have been removed

* Corresponding author. Institut für Experimentalphysik, Freie Universität Berlin, Arnimallee 14, D-14195 Berlin, Germany. Tel.: +49 (30)838 53047; fax: +49 (30)838 56081.
E-mail address: antonkin@physik.fu-berlin.de (M.L. Antonkine).
[1] On leave from the Photochemistry Center of the Russian Academy of Sciences, Novatorov St. 7a, 117421 Moscow, Russia.

0005-2728/$ - see front matter © 2007 Elsevier B.V. All rights reserved.
doi:10.1016/j.bbabio.2007.02.003

amino acid in the catalytic activity was clarified by the use of chemical rescue techniques.

Cysteine is one of the rarest and yet one of the most important amino acids in proteins because the thiolate side chain is capable of taking roles in structure [30], in acid–base chemistry [31], in chemical catalysis [32], in sensing and regulation [33], in radical chemistry [34], and as a ligand to a wide variety of prosthetic groups [35]. The latter role represents a particularly important function, especially in electron-transfer proteins. Proteins that contain mono-Fe and simple [2Fe–2S], [3Fe–4S], and [4Fe–4S] clusters employ almost exclusively thiolate ligands from Cys residues (the most notable exception includes Rieske [2Fe–2S] clusters, which employ two Cys and two His residues [36]). Yet, in spite of their importance, there are no reports in which chemical rescue techniques have been proven to restore the activity of site-modified Cys residues in proteins. Because of potential applications for modifying and controlling electron transfer processes, one of the most exciting uses of the technique would be to rescue the assembly of iron–sulfur clusters in ferredoxin variants and synthetic model proteins in which one or more of the ligating Cys residues has been removed.

Two of the authors of this paper (DAB and JHG) proposed earlier that *in vitro* a $[4Fe–4S]^{1+,2+}$ cluster may have been *inadvertently* rescued by 2-mercaptoethanol in site-modified variants of PsaC, a protein similar to bacterial dicluster ferredoxins and which is bound to photosystem (PS) I of green plants, algae and cyanobacteria [37–41]. PsaC is a 9.3 kDa polypeptide that contains two consensus C(I)xxC(II)xxC(III)xxxC(IV)P sequences, which bind two $[4Fe–4S]^{2+,1+}$ clusters termed F_A and F_B. PsaC is presumed to have evolved from a bacterial dicluster ferredoxin [42] by the addition of a C-terminal extension and by the insertion of five amino acids in the so-called Z-loop, which is located between the two consensus $[4Fe–4S]^{1+,2+}$ cluster binding sites. The three-dimensional solution structure of recombinant, unbound PsaC has also been solved by NMR [43] (PDB entry 1K0T), and the three-dimensional structure of PsaC has also been solved by X-ray crystallography as part of the PS I crystal structure [44] (PDB entry 1JB0). As predicted from the primary structure, the regions immediately surrounding the two [4Fe–4S] clusters in PsaC and in bacterial dicluster ferredoxins are highly similar in structure [43–45].

The goal of our previous work was to locate the binding sites of the spectroscopically distinguishable F_A and F_B clusters relative to the crystallographic axis of the protein (reviewed in [46]). In order to alter the EPR properties of the iron–sulfur clusters, two variants of PsaC, Cys13X (X=Gly, Ala, Ser or Asp) and Cys50X (X=Gly, Ala, Ser or Asp), were constructed [38–41,47].[2] Ser and Asp contain a side group that could potentially provide an oxygen ligand to an Fe atom, whereas Gly and Ala do not. Three possible outcomes of this experimental strategy were imagined: (1) an empty site would result from the inability of a $[4Fe–4S]^{1+,2+}$ cluster to assemble in the modified site; (2) the missing Cys ligand at the modified site would lead to a presence of a $[3Fe–4S]^{0,1+}$ cluster; or (3) a [4Fe–4S] cluster with altered redox and/or spectroscopic properties would assemble in the modified site. The PsaC variants were expressed in *Escherichia coli*, the apo-proteins were purified, and the iron–sulfur clusters were reinserted using $FeCl_3$, Na_2S and 2-mercaptoethanol by a procedure similar to that described in [48]. It is known that $[4Fe–4S]^{1+,2+}$ clusters self-assemble in such a reaction mixture [49]. These clusters can be inserted into apo-PsaC *via* a facile ligand exchange mechanism, which is probably similar to that observed earlier with synthetic analogs of iron–sulfur proteins, between the Cys residues in the protein and 2-mercaptoethanol [50]. When the reconstituted Cys13X (X=Gly, Ala, Ser or Asp) variants were reduced with sodium hydrosulfite, the EPR spectrum of each variant showed simple axial-like resonances characteristic of F_A^- in the $g=2$ region; however, resonances from the F_B^- cluster were not observed. Conversely, when the Cys50X (X=Gly, Ala, Ser or Asp) variants were reduced with sodium hydrosulfite, their EPR spectra showed simple, axial-like resonances characteristic of F_B^- in the $g=2$ region; however, resonances from the F_A^- cluster were not observed. Together with the known structure of dicluster ferredoxins, these results identified Cys residues 10, 13, 16 and 57 as ligands to F_B and Cys residues 20, 47, 50 and 53 as ligands to F_A [46]. Hence, F_B was found to be equivalent to Cluster I and F_A was found to be equivalent to Cluster II of bacterial dicluster ferredoxins.

When the PsaC variants were rebound onto P700-F_X cores and reduced either chemically or photochemically, the reconstituted PS I complexes showed complex EPR spectra characteristic of two magnetically-interacting $[4Fe–4S]^{1+}$ clusters, that were similar, although not identical, to wild-type PsaC. These results implied that the F_B cluster was present in the C13X variants and that the F_A cluster was present in the C50X variants. To explain these results, it was proposed that the ground spin state of the reduced [4Fe–4S] cluster in the altered site of unbound PsaC differed from that for the wild-type protein, making it difficult to observe by EPR. Furthermore, it was proposed that, when the C13X and C50X variants were bound the P700-F_X cores, the altered environment forced a crossover to the more typical $S=1/2$ ground spin state. Jung et al. [41] proposed that 2-mercaptoethanol, a reagent used in the reconstitution protocol, was retained as an external rescue ligand to the $[4Fe–4S]^{2+,1+}$ cluster in the modified site.

In spite of the implied presence of F_A and F_B in these reassembled PS I complexes, confirmation of the presence of two, intact $[4Fe–4S]^{1+,2+}$ clusters and the identification of the ligand in the modified site of the *unbound* PsaC variants was lacking. Here, in studies with the C13G/C33S PsaC variant, we provide definitive experimental evidence that validates the chemical rescue hypothesis. In this study, no *a priori* assumptions were made about the number or type(s) of iron–sulfur clusters, or about the identity of the ligand (if any) in the modified site of the C13G/C33S variant. Accordingly, the experiments unfold as a series of questions that, when approached experimentally, allow definitive conclusions to be

[2] Note that in previous studies the numbering of amino acids was based on the sequence of the *psaC* gene. The derived protein sequence therefore included the N-terminal methionine residue. This methionine is cleaved when PsaC is expressed in cyanobacteria or over-expressed in *Escherichia coli*. Here, we use the numbering based on the sequence of the expressed protein, which is one amino acid shorter.

reached about the number and type of iron–sulfur clusters in this PsaC variant and about the identity of the ligand to the iron–sulfur cluster in the modified site. The prospects for extending the findings described here to manipulate other members of the bacterial dicluster ferredoxin superfamily are discussed.

2. Materials and methods

2.1. Sample preparation and sample reduction

Synechococcus sp. PCC 7002 PsaC and its C13G/C33S variant were overproduced in *E. coli* and purified, and the iron–sulfur clusters were reconstituted using a previously-described procedure [43,48,51,52]. Unless specified, all procedures were carried out under anaerobic conditions. A slight modification was used when aryl thiolates were used in the iron–sulfur insertion protocol [53]. In this case 4-fluorothiophenol was dissolved in an ethanol/buffer solution (50%/50% v/v) prior to addition to the reconstitution mixture. After insertion of the iron–sulfur clusters, the samples were washed three times by concentration and dilution with 50 mM Tris–HCl, pH 8.3 by using a Centricon-3 centrifugal concentration device (YM-3 membrane; Millipore, Billerica, MA) at 3000×*g*. The resultant concentrated sample was purified by gel permeation chromatography on a Sephadex G-25 column equilibrated with 50 mM Tris–HCl, pH 8.3 in order to remove remaining iron, sulfide, and/or 2-mercaptoethanol. The brown-colored fraction was collected and concentrated. Prior to EPR measurements, the pH of the samples were adjusted to 10.0 by addition of 1 M glycine buffer, and the iron–sulfur clusters were reduced by addition of 1 mg of sodium hydrosulfite. Alternatively, the chemical reduction was carried out by addition of 3 mg of solid borohydride to the sample at pH 8.3, followed by quick freezing.

2.2. Ellman's assay for the number of free thiols

To ensure the presence of free thiols, apo-proteins were purified in the presence of 20 mM 2-mercaptoethanol. After purification, samples were dialyzed against degassed, argon-purged 50 mM Tris–HCl, pH 8.3, 20 mM NaCl buffer. The dialysis procedure was repeated three times over a period of 24 h to ensure complete removal of the 2-mercaptoethanol.

The number of Cys residues in the wild-type PsaC apo-protein and the C13G/C33S variant was determined using Ellman's reagent [54,55]. Briefly, 5,5′-Dithio-*bis*-(2-nitrobenzoic acid) (DTNB) solution (200 μl) was added to 1 M Tris–HCl buffer, pH 8.3 (100 μl), protein solution (10 μl) and water (690 μl). The sample was allowed to stand in the dark at room temperature for 1 h, and the absorbance was measured at 412 nm. A standard curve was prepared using 2-mercaptoethanol. The extinction coefficient of DTNB is 13,600 M^{-1} cm^{-1} at 412 nm [55].

2.3. Non-heme iron and acid-labile sulfide assays

The non-heme iron content of wild-type PsaC and the C13G/C33S variant were measured according to a previously defined protocol [56] with minor modifications. A 300 μL aliquot of PsaC in 50 mM Tris–HCl (pH 8.3) was added to 300 μL of reagent A (4.5% sodium dodecyl sulfate and a 1.5% saturated solution of sodium acetate) and 300 μL of reagent B (273 mM ascorbic acid, 8.45 mM sodium meta-bisulfate, and a 6.6% saturated solution of sodium acetate), and the mixture was incubated at 37 °C for 15 min. A total of 15 μL of reagent C [36 mM 3-(2-pyridyl)-5,6-di(2-furyl)-1,2,4-triazine-5′,5″-disulfonic acid disodium salt, also known as ferene] was added, and the absorbance was measured at 593 nm. The standard curve was constructed from a freshly prepared solution of $Fe(NH_4)_2(SO_4)_2 \cdot 6H_2O$.

The acid-labile sulfide content of wild-type PsaC and the C13G/C33S variant were determined colorimetrically after conversion into methylene blue by a reaction with 2,3-dimethylphenylenediamine [57]. Briefly, 2.0 ml of Zn acetate (1%, w/v) and 0.1 ml of NaOH (12%, w/v) were added to a sample (2 ml) in a 15-ml Teflon-capped tube. After 20 min, 1.0 ml of dimethylphenylenediamine (1% w/v, in 5 M HCl) was added, followed by addition of 200 μl of $FeCl_3$ (0.023 M in 1.2 N HCl). The samples were vortexed briefly, and after incubation in the dark for 2.5 h, hexanol (3.0 ml) was added, along with saturating concentrations of potassium chloride. The sample was vortexed briefly and allowed to stand until the two phases separated (typically 5 to 10 min). The methylene blue quantitatively partitions into the hexanol layer. The absorbance was measured at 660 nm. A standard curve was prepared using a freshly prepared solution of sodium sulfide. The extinction coefficient of methylene blue is 6000 M^{-1} cm^{-1} at 400 nm [54].

2.4. Optical absorption and resonance Raman spectroscopy

The optical absorbance spectra of wild-type PsaC and its C13G/C33S variant were measured between 260 nm and 700 nm in a tightly sealed quartz cuvette and were acquired with a Cary 50 UV-Vis spectrometer.

Resonance Raman spectra were recorded at 77 K using a conventional scanning Raman instrument equipped with a Spex 1403 double monochromator (with a pair of 1800 grooves/mm gratings), a Hamamatsu 928 photomultiplier detector under the control of a Spex DM3000 microcomputer system [58], and lines from a Coherent 90-6 Ar^+-ion laser. Back-scattered photons were collected directly from the surface of a frozen protein solution held in a vacuum on a liquid N_2-cooled cold finger [59]. Loading of the sample (~2–3 mM in 50 mM Tris–HCl, pH 8.3) onto the cold finger was performed in a glove bag under an argon atmosphere. No protein damage was observed at a laser power of 300 mW even after prolonged spectral data acquisition. Slit widths were set to 7 cm^{-1}, the spectrometer was advanced in 0.5-cm^{-1} increments, and integration times were 1 s per data point for all spectra. Multiple scans (32–40) were averaged to improve the signal-to-noise ratio and band positions were calibrated using the excitation wavelength. Slowly sloping baselines and ice Raman peaks (228, 314 cm^{-1}) were partially subtracted from the digitally collected spectra by using GRAMS/32 software (Thermo Galactic, Inc.) mounted on a PC computer. A GRAMS/32 CURVEFIT routine was used to deconvolute overlapping peaks into a combination of Gaussian curves. IGOR Pro (version 4.0) software (WaveMetrics, Inc., Lake Oswego, OR) was used to prepare the figure.

2.5. Mössbauer, EPR and NMR spectroscopy

Mössbauer data were recorded on an alternating, constant-acceleration spectrometer. The minimum experimental line width was 0.24 mm/s (full width at half-height). The sample temperature was maintained in an Oxford Instruments Variox cryostat. The gamma-source was ^{57}Co in Rh matrix (1.8 GBq). Isomer shifts are quoted relative to iron metal at 300 K.

X-band EPR experiments were performed using a Bruker ECS 106 X-band spectrometer operating with an ER/4012 ST resonator and an Oxford liquid helium cryostat. The magnetic field was calibrated using α,α′-diphenyl-β-picrylhydrazyl (DPPH) as standard. The temperature was controlled with an ITC4 Oxford temperature controller and the microwave frequency was measured using a Hewlett-Packard 5340A frequency counter.

^{19}F-NMR spectra were collected at 298 K without proton decoupling on a Bruker AMX2-500, which was operated at 470.566 MHz with a 5 mm inverse ^{19}F probe. Trifluoroacetic acid was employed as a standard. All NMR spectra were processed using Bruker XWINNMR software.

3. Results

3.1. Wild-type and C13G/C33S variants of PsaC contain 9 and 7 cysteines, respectively

Wild-type PsaC from the cyanobacterium *Synechococcus* sp. PCC 7002 contains nine Cys residues; eight are involved in ligating the two [4Fe–4S] clusters, F_A and F_B, and the ninth, located at position 33, is present as a free thiolate. In previous studies, the C33S variant of PsaC was shown to be spectroscopically and functionally equivalent to the wild-type protein [38]. We took advantage of this finding by constructing a C13G/C33S double mutant to remove a free cysteine that could interfere with spectroscopic studies (see below). The *psaC*

gene from *Synechococcus* sp. PCC 7002 was inserted into an expression vector as previously described [51], and the codons for Cys13 and Cys33 were changed to codons for Gly and Ser, respectively. Based upon the DNA sequence of the over-expression plasmid, the apo-protein form of C13G/C33S PsaC is predicted to contain seven Cys residues. Using purified recombinant proteins, Ellman's test confirmed the presence of 9.0±0.6 Cys residues in wild-type PsaC and 6.5±0.7 Cys residues in the C13G/C33S PsaC variant.

3.2. Wild-type and C13G/C33S variants of PsaC contain ~8 non-heme irons and ~8 acid-labile sulfides

Although no precedent exists for the occurrence of a single $[4Fe–4S]^{1+,2+}$ cluster in a ferredoxin that contains two $[4Fe–4S]^{1+,2+}$ consensus binding motifs, it was necessary to exclude the possibility that an iron–sulfur cluster might fail to assemble in the site-modified PsaC variant. This was accomplished, in part, by measuring the non-heme iron and acid-labile sulfide content of the reconstituted wild-type and variant proteins. Results from the colorimetric iron assay indicate the presence of 7.6±0.6 non-heme irons in the wild-type and 7.4±0.8 non-heme irons in the C13G/C33S variant. Results from the methylene blue assay indicate the presence of 7.6±0.2 acid-labile sulfides in wild-type and 7.7±0.6 acid labile sulfides in the C13G/C33S variant. Thus, the same iron content is found for both the wild-type and the C13G/C33S variant of PsaC. The precision of the measurements does not allow one to distinguish between the presence of two $[4Fe–4S]^{1+,2+}$ clusters or one $[3Fe–4S]^{0+,1+}$ and one $[4Fe–4S]^{1+,2+}$ cluster in the variant protein. However, we can conclude that C13G/C33S variant of PsaC contains two cubane iron–sulfur clusters.

Wild-type PsaC and the C13G/C33S PsaC variant contain the same number of aromatic amino acid residues. Therefore, the ratio between the absorption at 400 nm, which is due to metal-to-ligand charge transfer bands, and the absorption at 280 nm, which is predominantly due to aromatic amino acids, will be a function of the number of $[4Fe–4S]^{1+,2+}$ clusters in each protein. The optical absorption spectra (not shown) are highly similar, and in particular, the nearly identical values of the 280 nm to 400 nm ratio for wild-type PsaC (2.0) and the C13G/C33S variant (2.1) indicates that both proteins must contain the same number of cubane clusters. When both proteins were reduced with sodium hydrosulfite at pH 10.0, the absorbance decreased by one-half (data not shown) as typical for proteins that contain iron–sulfur cluster(s). Thus, the possibility that the C13G/C33S PsaC variant contains a single $[4Fe–4S]^{1+,2+}$ cluster and an empty site can be excluded.

3.3. The C13G/C33S PsaC variant does not contain a $[3Fe–4S]^{0+,1+}$ cluster

Resonance Raman (RR) spectroscopy provides a sensitive structural probe of iron–sulfur clusters in proteins [60] and allows different types of iron–sulfur clusters to be distinguished. The most thorough analysis of the RR spectrum for a protein-bound low-potential [4Fe–4S] cluster is that of the bacterial dicluster ferredoxin from *Clostridium pasteurianum* [30,59,61]. The RR bands have been rigorously assigned under effective D_{2d} symmetry by studies of synthetic analogues, ^{34}S and ^{54}Fe isotope shifts, and normal mode calculations. We take advantage of these assignments here in the study of PsaC and its C13G/C33S variant.

Fig. 1 shows a comparison of the low-temperature (77 K) RR spectra obtained with 488.0-nm excitation wavelength of oxidized wild-type PsaC (trace A) and the C13G/C33S PsaC variant (trace B). The RR spectrum of wild-type PsaC has an overall vibrational pattern that is unique to proteins containing low-potential [4Fe–4S] clusters. In particular, it is dominated by a band at 336 cm^{-1} arising from the vibrational marker of the [4Fe–4S] core structure, the A_1 bridging breathing $\nu(FeS^b)$ mode in the limiting T_d symmetry [30,61,62]. Assignments of RR lines of *C. pasteurianum* ferredoxin are extended to the vibrational modes observed for oxidized wild-type PsaC, as shown in Table 1. There are a number of differences in the two spectra. The 391-cm^{-1} band in wild-type PsaC is attributed to both A_1 $\nu(FeS^t)$ and T_2 $\nu(FeS^b)$ modes that arise from coincidental frequencies, whereas these modes are well separated in *C. pasteurianum* ferredoxin. Also, the intensity of the 287-cm^{-1} band in wild-type PsaC is larger than that observed in the spectrum of *C. pasteurianum* ferredoxin.

The RR spectrum of the C13G/C33S PsaC variant is similar both in relative intensities and in frequencies to that of wild-type PsaC. Both proteins exhibit the characteristically intense, A_1 cluster-breathing RR band that is centered near 336–337 cm^{-1}. There is a direct, one-to-one correspondence of spectral features between the C13G/C33S PsaC variant and wild-type PsaC.

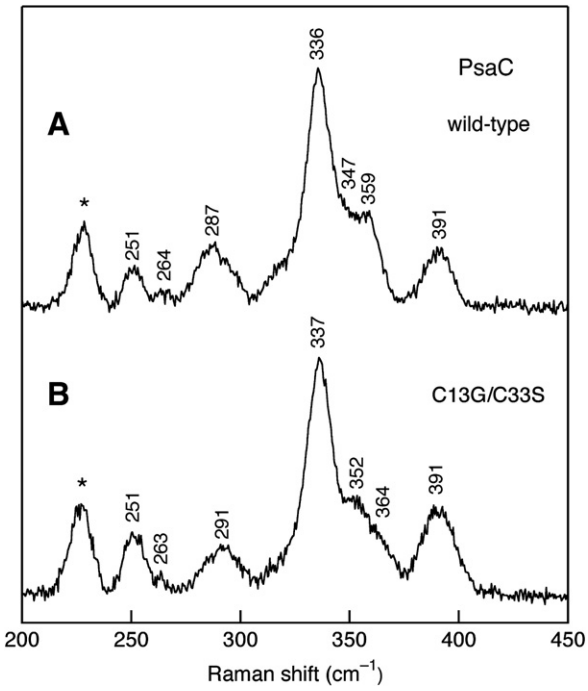

Fig. 1. Low-temperature (77 K) resonance Raman spectra of wild-type (A) and C13G/C33S (B) PsaC obtained in the 200- to 450-cm^{-1} region with 488.0 nm excitation wavelength, ~300 mW laser power, and 7 cm^{-1} slit widths. (*) Denotes ice band.

Table 1
Resonance Raman frequencies (cm^{-1}) and assignments for $[4Fe–4S]^{2+}$ clusters in *C. pasteurianum* ferredoxin (Fd)[a], wild-type PsaC, and the C13G/C33S PsaC variant

Mode (D_{2d}) (T_d)	*C. pasteurianum* Fd [a]	PsaC [b]	C13G/C33S [b]
Mainly terminal ν(FeS)			
A_1	395 (3.9)	391 [c]	391 [c]
E (T_2)	363 (2.0)	359	364
B_2 (T_2)	351 (0.7)	347	352
Mainly bridging ν(FeS)			
E (T_2)			
B_2 (T_2)	380 (5.6)	391 [c]	391 [c]
A_1	338 (7.0)	336	337
A_1 (E)	298 (4.9)		
		287	291
B_1 (E)	276 (5) [c]		
E (T_1)	276 (5) [c]		
A_2 (T_1)	266 (4.0)	264	–
E (T_2)			
B_2 (T_2)	251 (6.2)	251	251

[a] Data and vibrational assignment with ^{34}S isotope shifts in parentheses [$\nu(^{32}S)-\nu(^{34}S)$] from Czernuszewicz et al. [61].
[b] This work.
[c] Overlapping bands.

Minor differences were observed in the 350 to 365 cm^{-1} region, where the frequencies of the C13G/C33S PsaC variant were upshifted by 5 cm^{-1} relative to those of wild-type PsaC, and in the 280 to 300 cm^{-1} region, where the band envelopes appear to have a slightly different shape. The nearly constant vibrational frequencies for both wild-type and the C13G/C33S PsaC variant, in particular the A_1 bridging vibration at ~337 cm^{-1}, indicates that the structure of the [4Fe–4S] clusters is not significantly altered in the C13G/C33S variant.

A $[3Fe–4S]^{0,1+}$ cluster gives rise to $\nu(FeS^b)$ bands at ~265, ~285, and 347 cm^{-1}, which is the most prominent band, and two or three $\nu(FeS^t)$ bands between 360 and 400 cm^{-1} [63,64]. None of these features are present in the RR spectra of wild-type PsaC and the C13G/C33S variant, and hence it can be concluded that $[3Fe–4S]^{0,1+}$ clusters are not present in both samples.

This assessment is further supported by EPR studies. The spectra of both the as-reconstituted wild-type PsaC and its C13G/C33S variant lack the typical $g=2.01$ and 1.98 resonances that arise from an $S=1/2$ $[3Fe–4S]^{1+}$ cluster, and the broad $g=11.5$ resonance from an $S=2$, $[3Fe–4S]^0$ cluster after chemical reduction (data not shown).

The enhanced RR bands associated with bridging and terminal iron–sulfur stretching vibrations are distinctive for different structural types of iron–sulfur clusters. The appearance of an intense band in the 281 to 291 cm^{-1} region is a characteristic feature that distinguishes [2Fe–2S] clusters from [4Fe–4S] clusters. EPR measurements give no evidence of a [2Fe–2S] cluster in the reduced C13G/C33S PsaC. The formation of a [2Fe–2S] cluster from the degradation of a [4Fe–4S] cluster has never been observed in PsaC. The results of acid-labile sulfide assay and optical spectroscopy also show that formation of [2Fe–2S] cluster could be clearly excluded in C13G/C33S PsaC. Thus, the combination of biochemical, RR and EPR data allows us to conclude that the C13G/C33S PsaC variant does not contain a $[3Fe–4S]^{0,1+}$ cluster or a $[2Fe–2S]^{1+,2+}$ cluster.

3.4. The EPR spectrum of the reduced C13G/C33S PsaC variant at $g\sim2$ is that of a single $[4Fe–4S]^{1+}$ cluster in the $S=1/2$ ground state

The iron–sulfur clusters in wild-type PsaC can be reconstituted using aryl or alkyl thiolates, including 2-mercaptoethanol [40], thiophenol [53], 2,2,2-trifluoroethanethiol or 4-fluorothiophenol (this work). (The use of the fluorinated aryl and alkyl thiolates is a precondition for the NMR studies described below.) The EPR spectrum in the $g=2$ region of the C13G/C33S PsaC variant, which had been reconstituted with 4-fluorothiophenol and chemically reduced, is identical to the spectra obtained previously for C13X (X=A, G, D, S) variants that had been reconstituted with the 2-mercaptoethanol [38,40,53]. The axial-like spectrum (Fig. 2A, solid line) appears to result from a single $[4Fe–4S]^{1+}$ cluster in the $S=1/2$ ground state with no indication of spin–spin interaction with a second $[4Fe–4S]^{1+}$ cluster. The spectrum is similar, although not identical, to the spectrum of C50X (X=A, G, D, S) reconstituted with 2-mercaptoethanol. The C13X and C50X variants are subtly different: the C13X variants exhibit a high-field trough at $g=1.89$ and have a slightly narrower linewidth, while the C50X variants exhibit a high-field trough at $g=1.90$ and have a slightly broader linewidth (see Ref. [46]).

If the reduced state C13G/C33S variant contains two $[4Fe–4S]^{1+}$ clusters but only one is in the $S=1/2$ ground state, then the integrated spin concentration around $g=2$ should be one-half of that of wild-type PsaC. The wild-type protein and the C13G/C33S variant were compared on the basis of an equivalent optical absorbance at 400 nm of the oxidized samples. Note that we can achieve quantitative reduction of the sample (see below). The integrated spin intensity between 3200G and 3800G in the C13G/C33S variant was found to be 49% that of the integrated spin intensity of wild-type PsaC (Fig. 2A, solid vs. dashed lines). Thus, the resonances around $g=2$ in the C13G/C33S variant appear to be derived from a single $[4Fe–4S]^{1+}$ cluster.

3.5. All $[4Fe–4S]^{2+}$ cluster(s) are chemically reduced in the C13G/C33S PsaC variant

One possible reason that only one of the two [4Fe–4S] clusters is detected in the C13G/C33S variant of PsaC is that the altered ligand environment in the modified site drives the [4Fe–4S] cluster sufficiently electronegative that it cannot be reduced with sodium hydrosulfite at pH 10 or with sodium borohydride at pH 8.3. Mössbauer spectroscopy can distinguish between different type(s) of iron–sulfur clusters, and can also discriminate between their oxidation state(s).

Fig. 3A shows the zero-field Mössbauer spectrum of the as-reconstituted C13G/C33S PsaC variant. Most of the signal (84%) can be assigned to a quadrupole doublet with isomer-shift and quadrupole-splitting parameters typical for an oxidized, low-potential [4Fe–4S] cluster [65] (for review see

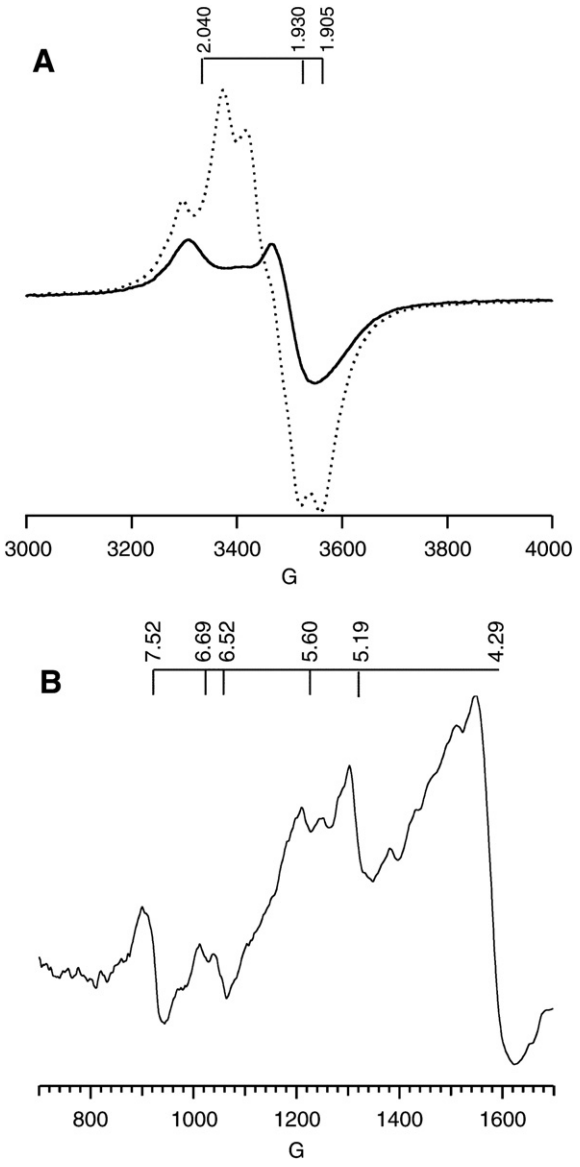

Fig. 2. (A) The $g=2$ region of the EPR spectrum of the wild-type (dashed line) and the C13G/C33S PsaC variant (solid line) reconstituted with 2-mercaptoethanol. The identical spectrum is detected when the C13G/C33S variant is reconstituted with 4-fluorothiophenol. The wild-type and variant samples were measured at equivalent optical absorbance at 400 nm. The samples were reduced with sodium hydrosulfite at pH 10.0. EPR conditions: temperature 16 K, microwave power 126 mW, microwave frequency, 9.48 GHz, modulation amplitude 10 G. (B) Low field region of the EPR spectrum of the C13G/C33S PsaC variant reconstituted with 4-fluorothiophenol. The sample was reduced with sodium borohydride at pH 8.3. The identical spectrum is detected when the C13G/C33S variant is reconstituted with 2-mercaptoethanol and reduced with sodium hydrosulfite at pH 10.0. EPR conditions: temperature 5 K, microwave power 200 mW, modulation amplitude 10 G.

[66]). This result agrees with the conclusion reached on the basis of RR spectroscopy and EPR spectroscopy that only $[4Fe–4S]^{1+,2+}$ clusters are present in the C13G/C33S PsaC variant. A small amount of the signal (11%) is attributed to adventitiously bound iron(II) and less than 5% to a super-paramagnetic iron oxide species, both of which are frequently found in Mössbauer samples of *in vitro* reconstituted iron–sulfur proteins.

After reduction of the C13G/C33S PsaC variant with either sodium borohydride at pH 8.3 (not shown) or sodium hydrosulfite at pH 10 (Fig. 3B), the isomer-shift and quadrupole-splitting parameters increase in magnitude, in agreement with the stronger ferrous character of a valence-delocalized cubane $[4Fe–4S]^{1+}$ electronic system. The broadening of the spectrum is caused by the magnetic hyperfine interactions between the electronic spin and the ^{57}Fe nuclei, and these changes are also consistent with the expected behavior of $[4Fe–4S]^{1+}$ clusters [65] (for review see [66]). The presence of an oxidized $[4Fe–4S]^{2+}$ cluster remaining under these reducing conditions can thus be clearly excluded. A comprehensive interpretation of the Mössbauer spectrum of the reduced C13G/C33S variant with an applied magnetic field was precluded by the presence of the super-paramagnetic iron species in the sample. Nevertheless, these results indicate that under the experimental conditions employed, both chemical reduction protocols completely reduce the $[4Fe–4S]^{2+}$ clusters in the C13G/C33S PsaC variant to the +1 oxidation state.

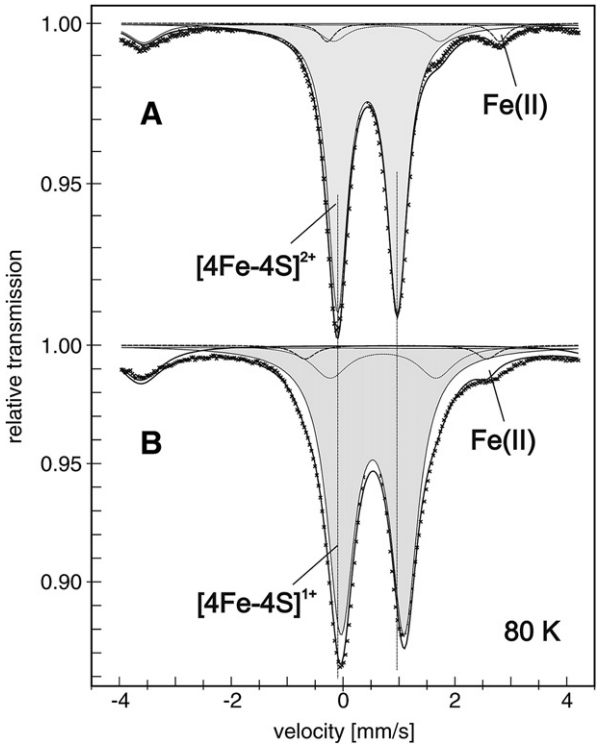

Fig. 3. A zero-field Mössbauer spectrum at 80 K of C13G/C33S PsaC reconstituted with $^{57}FeCl_3$ in oxidized (A) and reduced (B) forms. The experimental spectrum (marks x) was simulated by using a superposition of three components which we assigned to the following species: first, a Lorentzian doublet from oxidized [4Fe–4S] cluster (A) $\delta=0.44$ mm/s, $\Delta E_Q=1.07$ mm/s, Line Width=0.43 mm/s, relative intensity 84%; (B) $\delta=0.53$ mm/s, $\Delta E_Q=1.13$ mm/s, Line Width=0.58 mm/s, relative intensity 78% (thin solid line, area marked in gray); second, a Lorentzian doublet from an iron (II) impurity (A) $\delta=1.26$ mm/s, $\Delta E_Q=3.08$ mm/s, Line Width=0.34 mm/s, relative intensity 11%, (B) $\delta=1.0$ mm/s, $\Delta E_Q=3.25$ mm/s, Line Width=0.45 mm/s, re. intensity 4% (dashed line); and third, a broad six-line-pattern from super-paramagnetic iron oxide fit with (A) $\delta=0.5$ mm/s, Line Width=0.7 mm/s, relative intensity 5%, (B) $\delta=0.71$ mm/s, Line Width=0.8 mm/s, relative intensity 18% (dotted line).

3.6. The EPR spectrum of the reduced C13G/C33S variant shows evidence for a [4Fe–4S]$^{1+}$ cluster in the $S \geq 3/2$ ground spin state

Another reason that the second [4Fe–4S]$^{1+}$ cluster may not be visible in the $g=2$ region of the EPR spectrum is that the altered ligand environment causes a change in the magnetic coupling of the iron atoms, resulting in crossover to one or more higher ground spin states. Although earlier studies mentioned a weak set of resonances around $g=5$ to 6 in the C50X variant [38,40], in the present work, the availability of significantly higher protein concentrations and a more efficient reduction protocol allowed EPR signals to be recorded with a much higher signal-to-noise ratio. This permitted the observation of resonances that had previously been below the level of detection. Fig. 2B shows the EPR spectrum of the chemically-reduced C13G/C33S PsaC variant in the 800 to 1650 G region. Signals with apparent g-values of 7.5, 6.7, 6.5, 5.6 and 5.2 are readily seen (the resonance at $g=4.3$ is derived from a small population of adventitiously bound, octahedrally-coordinated Fe^{3+} in the $S=5/2$ ground spin state). Although these signals are assigned to a [4Fe–4S]$^{1+}$ cluster, it is not possible to identify a particular spin manifold by using the typical rhombograms for $S=5/2$, 7/2 or even higher spin states. This may be due to an unfavorable zero-field splitting constant of the cluster spin manifold in the low or intermediate exchange regime, for which rhombogram approximations are not valid ($D >> g\mu_B B$). In spite of this limitation, these data clearly indicate the presence of a [4Fe–4S]$^{1+}$ cluster with an $S \geq 3/2$ ground spin state. We conclude that the reduced C13G/C33S PsaC variant contains a [4Fe–4S]$^{1+}$ cluster with $S=1/2$ ground spin state in the unmodified site (Fig. 2A) and a [4Fe–4S]$^{1+}$ cluster with $S \geq 3/2$ ground spin state in the modified site (Fig. 2B).

3.7. Chemical rescue of the [4Fe–4S]$^{1+,2+}$ cluster in the C13G/C33S variant by an external thiolate

If a [4Fe–4S]$^{1+,2+}$ cluster is present in the modified site of the C13G/C33S PsaC variant, the identity of the ligand that replaces the Cys13 thiolate is the essential question, since glycine has no side chain. One possibility is oxygen from either water or hydroxide ion, both of which have been implicated in ligation to the labile iron in aconitase [67]. Another possibility is that 2-mercaptoethanol, a reagent used during the iron–sulfur reconstitution protocol, provides the ligand. This possibility might arise from the inability of glycine to displace 2-mercaptoethanol during the ligand exchange reaction that leads to the insertion of the [4Fe–4S]$^{1+,2+}$ clusters into the C13G/C33S apoprotein. Note that Cys 13, which was replaced by Gly, is closest to the surface of the protein (see PDB entry 1K0T, [43]). To provide support for an external thiolate ligation of the [4Fe–4S] cluster in the modified site of PsaC, we relied on the fact that a fluorinated organic ligand would be expected to experience a large contact shift and line broadening when bound to a paramagnetic cluster [68–70]. We also relied on the fact that none of twenty amino acids has a fluorine atom as part of its structure, and that the 100% natural abundance of the NMR-detectable $I=1/2$ ^{19}F nucleus would negate the need for enrichment procedures; it was also to our advantage that the NMR sensitivity of the ^{19}F nuclei approaches that for protons.

The ^{19}F-NMR spectrum of the C13G/C33S PsaC variant, which had been reconstituted with an aryl thiolate, 4-fluorothiophenol, exhibits a broad peak at −37.6 ppm and a sharp peak at −48.1 relative to the trifluoroacetic acid standard (Fig. 4A). As a control, the iron–sulfur cluster-free apoprotein of PsaC was aerobically incubated with 4-fluorothiophenol. The ^{19}F-NMR spectra of this control sample (Fig. 4B) showed sharp

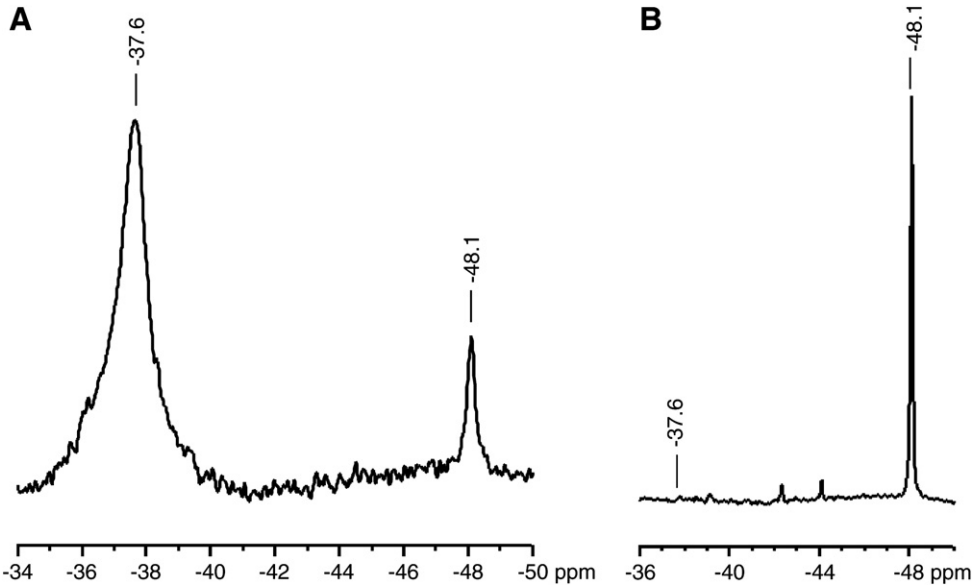

Fig. 4. (A) ^{19}F-NMR spectra of 2 mM PsaC variant C13G/C33S reconstituted with 4-fluorothiophenol and (B) ^{19}F-NMR spectra of 2 mM apoPsaC variant C13G/C33S incubated aerobically with 4-fluorothiophenol. Two low intensity peaks in the control sample arise due to contaminants in commercially available 4-fluorothiophenol.

peak at −48.1 ppm, which is attributed to non-specifically bound 4-fluorothiophenol. Thus, the hyperfine contact-shifted −37.6 ppm peak derives from 4-fluorothiophenol bound to the $[4Fe–4S]^{2+}$ cluster. The broad linewidth of this signal provides further evidence that the fluorinated ligand is bound to a paramagnetic center. The ^{19}F-NMR spectrum of the C13G/C33S PsaC variant that was reconstituted with an alkyl thiolate, 2,2,2-trifluoroethanethiol, showed a broad peak at 9.4 ppm and a sharp peak at 7.6 ppm (data not shown). When the iron–sulfur cluster-free apoprotein was aerobically incubated with 2,2,2-trifluoroethanethiol, the sharp peak at 7.6 ppm was similarly assigned to non-specifically bound thiol, and the broad, hyperfine contact-shifted peak at 9.4 ppm was assigned to a 2,2,2-trifluoroethanethiol ligand to the $[4Fe–4S]^{2+}$ cluster.

These results can be compared with ^{19}F-NMR data obtained previously from model $[Fe_4S_4(Sr)_4]^{2-}$, $[Fe_4S_4(Sr)_4]^{3-}$ and $[MoFe_3S_4(SR)_4L]^{3-}$ (R=*p*-C_6H_4F, $C_6H_4CF_3$; L=3,6-dialylcatecholate) compounds and from core-extrusion experiments on proteins that contain simple and complex iron–sulfur clusters [69,71]. Although a model $[4Fe–4S]^{2+}$ cluster bound by three Cys and a single 4-fluorothiophenol has not yet been synthesized, Mascharak et al. [71] reported that, upon attachment of four 4-fluorothiophenol ligands to a $[4Fe–4S]^{2+}$ cluster or three 4-fluorothiophenol ligands to a $[1Mo–3Fe–4S]^{2+}$ cluster (the Mo ligand is dialylcatecholate), the ^{19}F-NMR spectra show contact-shifted resonances attributed to the cluster-bound fluorinated aryl thiolate. The ^{19}F resonance of a thiolate that ligates an iron–sulfur cluster is also much broader than ^{19}F resonances of unbound or non-specifically bound fluorinated thiolates. Similar to results reported for model compounds and for iron–sulfur core extrusion experiments [69,71], we detect a broad contact-shifted resonance arising from the thiolate bound to the [4Fe–4S] cluster in the C13G/C33S variant.

To our knowledge, there are no reports of model $[4Fe–4S]^{1+,2+}$ clusters ligated by alkyl thiolates that have also been studied by ^{19}F-NMR spectroscopy. Therefore, our interpretation of the results obtained upon reconstituting the C13G/C33S PsaC variant with 2,2,2-trifluoroethanethiol relies on a qualitative interpretation of ^{19}F-NMR results obtained for model compounds ligated by fluorinated aryl thiolates. When the C13G/C33S variant was reconstituted with 2,2,2-trifluoroethanethiol, a broad downfield-shifted resonance was also observed. This implies that an alkyl thiolate, which is similar to 2-mercaptoethanol, similarly serves as a ligand to the $[4Fe–4S]^{2+}$ cluster. The chemical-rescue hypothesis for bacterial dicluster ferredoxins is thus validated by the experimental evidence that an external thiolate is directly bound to the [4Fe–4S] cluster in the modified site of the C13G/C33 PsaC variant.

4. Discussion

4.1. The existence of $[4Fe–4S]^{1+}$ clusters with ground spin states of $S \geq 3/2$

Naturally-occurring ferredoxins that contain reduced [4Fe–4S] clusters with ligands other than Cys often show ground spin states other than $S=1/2$. The reduced [4Fe–4S] cluster in *Pyrococcus furiosus* ferredoxin, which is ligated by three Cys and one Asp residue, exists in a spin mixture of $S=3/2$ (80%) and $S=1/2$ (20%) ground states [72]. Ferredoxin III from *Desulfovibrio africanus* contains a $[4Fe–4S]^{1+,2+}$ cluster, which is ligated by four Cys residues and a $[4Fe–4S]^{1+,2+}$ cluster, which is ligated by three Cys and one Asp residue; in reduced state this ferredoxin contains approximately equal proportions of a $[4Fe–4S]^{1+}$ cluster with an $S=1/2$ ground state and a $[4Fe–4S]^{1+}$ cluster with an $S=3/2$ ground spin state [73]. The possibility that both clusters in ferredoxin III adopt an $S=1/2$ and an $S=3/2$ ground spin state in some form of equilibrium was rejected in favor of the conclusion that the $S=3/2$ ground spin state is derived exclusively from the mixed-ligand $[4Fe–4S]^{1+}$ cluster. Indeed, alteration of the solvent induced by the addition of urea or ethylene glycol is sufficient to cause a spin state crossover between $S=1/2$ and $S=3/2$ in the Fe-only protein of nitrogenase from *Azotobacter vinelandii* [74]. While the presence of an oxygen-containing amino acid in *P. furiosus* ferredoxin and *D. africanus* ferredoxin III does not make a perfect analogy with the Gly variant of PsaC that has been rescued with an external thiolate, it is nevertheless the case that in both instances the substitution is also at position C(II) of the C(I) xxC(II)xxC(III)xxxC(IV)P consensus [4Fe–4S] binding motif.

Synthetic models of low-potential [4Fe–4S] clusters with different spin states have also been studied [75]. To date, no clear correlation has been found between cluster structure and its spin state because no firm relationship exists between the distortion of T_d symmetry, observed in both synthetic and biological $[4Fe–4S]^{1+,2+}$ [61] clusters [75,76], and the chemical nature of the ligands to the cluster. For instance both alkyl and aryl thiolates can produce "spin-admixed" $[4Fe–4S]^{1+}$ clusters *in vitro*. Nevertheless, Carney and coworkers [77] showed that the ground spin state of a synthetic $[4Fe–4S]^{1+}$ cluster depends on the ligand environment and that all of the compounds in frozen solutions were physical mixtures of $S=1/2$ and 3/2 spin states, with axial-like resonances at $g=2.05–2.03$ and 1.94–1.92 and broad, poorly resolved peaks around $g=5$. For alkylthiolate-ligated $[4Fe–4S]^{1+}$ clusters, the $S=3/2$ spin state became more prevalent as the side group on the thiolate became more bulky. It was concluded that the 'fine details of cluster structure and the accompanying stabilization of a ground spin state are enormously sensitive to environment'. While we cannot be certain of the identity of the ground spin state(s) of the chemically-rescued $[4Fe–4S]^{1+}$ cluster in the modified site of the C13G/C33S PsaC variant, or indeed whether any $S=1/2$ ground state exists in the chemically-rescued $[4Fe–4S]^{1+}$ cluster, it appears that the alteration of the protein structure by the replacement of Cys with Gly, and the presence of the aryl or alkyl thiolate as an externally-supplied ligand, is sufficient to change the magnetic coupling among the iron atoms that results in the loss of the $S=1/2$ ground-state character.

4.2. Externally-supplied ligands to site-modified $[4Fe–4S]^{1+,2+}$ clusters

The $[4Fe–4S]^{1+,2+}$ cluster in the Asp-containing site of ferredoxin III from *D. africanus* readily loses an iron to form

a $[3Fe–4S]^{0,1+}$ cluster [73]. When the $[3Fe–4S]^{0,1+}$ cluster is transformed into a $[4Fe–4S]^{1+,2+}$ cluster by addition of an extra iron, a reversibly coordinated thiolate anion can be detected by voltammetry. While this finding constitutes a *bona-fide* chemical rescue of an iron–sulfur cluster by an external thiolate, it was unfortunately not possible to determine the resulting ground spin state of the all-thiol ligated $[4Fe–4S]^{1+}$ cluster because the high concentrations of 2-mercaptoethanol resulted in the degradation of the cluster [78]. Interestingly, when the Asp is replaced by a Cys, the ground spin state crosses over from $S=3/2$ to $S=1/2$ [79]. This again reinforces the point that the magnetic coupling between the iron atoms of the $[4Fe–4S]^{1+}$ cluster is highly sensitive to the identity of the ligand at position (II) of the consensus [4Fe–4S] binding motif.

The literature contains one instance in which a $[4Fe–4S]^{1+,2+}$ cluster is ligated to a synthetic peptide that contains fewer than four Cys residues. A stable $[4Fe–4S]^{1+,2+}$ cluster can be bound by a peptide, termed FdM, which consists of 16 amino acids including the C(I)xxC(II)xxC(III)xxxC(′IV)P consensus binding site [80,81]. Indeed, the EPR spectrum of the reduced [4Fe–4S] cluster is highly similar to that of the C13G/C33S variant described in this work. The EPR relaxation properties, *i.e.* microwave power and temperature dependence, are typical of a $[4Fe–4S]^{1+}$ cluster. The deletion of one Cys (I) or even two of the Cys (II & III) from the consensus binding site had virtually no effect on the EPR spectrum, although the yield of the latter was relatively low [80,81]. Notably, EPR signals characteristic of $S=3/2$ ground spin states were not observed in any of these samples. The authors of this study suggested that the cluster might be bound to the peptide variant with one or two hydroxyl ligands, that the $[4Fe–4S]^{1+,2+}$ cluster might be bound to the peptide variant with thiolate ligands provided by the 2-mercaptoethanol used in the reconstitution procedure, or that the $[4Fe–4S]^{1+,2+}$ cluster might be ligated between two peptides. Given that thiolate ligation is strongly preferred over oxygen ligation [46,82] and that aryl and alkyl thiolates have been shown experimentally to provide an external thiol ligand in the C13G/C33S PsaC variant (this work), we favor the suggestion that the $[4Fe–4S]^{1+,2+}$ cluster is rescued by 2-mercaptoethanol in the majority of the peptides.

4.3. An absence of magnetic interaction between $S=1/2$ and $S\geq 3/2$ [4Fe–4S] clusters in variant PsaC

Wild-type PsaC belongs to the class of bacterial dicluster ferredoxins, which show a so-called interaction spectrum around $g=2$ due to magnetic coupling between the two closely-spaced $S=1/2$ $[4Fe–4S]^{1+}$ clusters. This magnetic interaction is mostly dipolar in nature. The EPR spectrum of the C13G/C33S PsaC variant is different from that of reduced, wild-type PsaC in that its spectrum is virtually identical to that of a PsaC variant that has been engineered to contain only one low-potential [4Fe–4S] cluster [53] or to model peptides which bind a single low-potential [4Fe–4S] cluster [80,81]. Thus, the magnetic interaction between the $S=1/2$ $[4Fe–4S]^{1+}$ cluster and the $S\geq 3/2$ $[4Fe–4S]^{1+}$ cluster in the C13G/C33S PsaC variant is either too weak to be observed or there is no magnetic coupling. It should be noted that magnetic interaction would be even more difficult to detect in the high-spin F_B species because the appearance of the spectrum is determined by a large zero-field splitting, and the signals are spread over a wide range of the field axis.

The absence of magnetic interaction between two $[4Fe–4S]^{1+}$ clusters in the same protein is not unprecedented. When *Chromatium vinosum* (*C. vinosum*) ferredoxin was investigated by EPR, the spectra of the fully reduced and partially reduced samples were found to be very similar, consistent with an absence of magnetic interaction between the two $[4Fe–4S]^{1+}$ clusters [83]. However, when a more effective reduction protocol was used, a reinvestigation of the same protein at low temperatures revealed the magnetic interaction between the two $[4Fe–4S]^{1+}$ clusters [84]. Moreover, it was shown that the unusual EPR spectra previously attributed to both $[4Fe–4S]^{1+}$ clusters [83] actually belonged to a single $S=1/2$ $[4Fe–4S]^{1+}$ cluster. A temperature effect was found with the mixed-ligand $[4Fe–4S]^{1+}$ cluster when the C50D variant of PsaC, where the ligand in the modified site is presumed to be the oxygen from Asp. At temperatures at or above 15 K, the EPR spectrum of the reduced protein showed signals arising from the F_B $[4Fe–4S]^{1+}$ cluster only, while at lower temperatures, a complex spectrum was observed characteristic of magnetic interaction between the two $[4Fe–4S]^{1+}$ clusters F_A and F_B [46].

We can imagine a reason for the absence of a magnetic interaction between two $[4Fe–4S]^{1+}$ clusters in the fully reduced protein. It is possible that the strength of the magnetic interaction is a function of the distance and relative orientation of the mixed valence pairs that carry the unpaired electron in each of the two iron–sulfur clusters. If so, then the strength of the magnetic interaction may be a function of the location of the mixed- and equal-valence pairs in each of the two $[4Fe–4S]^{1+}$ clusters.

In the case of *C. vinosum,* significant structural differences are observed in the binding site of the second [4Fe–4S] cluster. It was proposed that this influences the distribution of mixed- and equal-valence pairs in one or both reduced [4Fe–4S] clusters in such a way that the magnetic interaction is weakened. In support of this proposal, Calzolai et al. [85] showed that a change in ligand Cys II in the consensus [4Fe–4S] cluster binding motif to Asp or Ser leads to changes in the distribution of mixed- and equal-valence pairs of the reduced [4Fe–4S] cluster in *P. furiosus* ferredoxin. It is possible that the relatively small structural change from a Cys thiolate to an external thiolate ligand in the C13S/C33G variant of PsaC could shift the position of the equal and mixed valence pairs in a manner similar to a change from S to O ligation in *C. vinosum* ferredoxin. This proposal will be tested in the C13S/C33G variant of PsaC with additional NMR studies, which are planned in the near future.

4.4. Exploitation of the chemical rescue of [4Fe–4S]$^{1+,2+}$ clusters in bacterial dicluster ferredoxins

The demonstration that a site-altered [4Fe–4S]$^{1+,2+}$ cluster can be rescued with an external thiolate suggests several new opportunities for modulating the properties of [4Fe–4S]$^{1+,2+}$ clusters as well as the proteins which contain them. One potential application of the chemical-rescue method would be to modulate the midpoint potentials of the F_A and F_B [4Fe–4S] clusters in C13G and C50G variants using aryl thiolates carrying various electron-withdrawing or electron-donating groups. Once such variants have been rebound to PS I core complexes, the forward and backward electron transfer rates could be correlated with the reduction potential of F_A and F_B. This information could provide new insights into the design features of the PS I reaction center that lead to its remarkably high quantum efficiency as well as the tolerance of PS I-bound iron–sulfur clusters to oxygen.

A second application of the chemical-rescue method would be to rescue the [4Fe–4S]$^{1+,2+}$ cluster ligand with a thiolate ligand attached to a synthetic electron acceptor, e.g., a viologen dye, *via* a spacer of variable length and/or chemical composition. Since viologen dyes have favorable optical absorption properties with large molar extinction coefficients as well as sharp EPR lines in the one-electron reduced state, the reduction of such dyes could easily be followed by both optical and EPR spectroscopy. The length and composition of the spacer could easily be varied to determine those molecular structures that maximize the rate and efficiency of electron transfer to the viologen acceptor molecule. This information might lead to new insights into the mechanism(s) of electron transfer reactions.

Finally, a third potential application of this technology would be to use the chemical rescue approach to tether two iron–sulfur cluster-containing proteins together *via* a *bis*-thiolate molecule to create a new pathway for electron transfer with high rate and efficiency between the selected partner proteins. The iron–sulfur clusters of many electron transfer proteins are located near the surface of those proteins, so that the intermolecular distance for electron transfer can be minimized when the two partner proteins are proximal. For example, in both Fe-only and Ni-Fe-hydrogenases, [4Fe–4S]$^{1+,2+}$ clusters occur very close to the surface of either the large subunit or the small subunit, respectively, in order to accept or deliver electrons to a soluble ferredoxin or flavodoxin donor/acceptor. By using appropriate thiolate-containing spacer moieties, one could in principle link two iron–sulfur proteins by chemically rescuing variant clusters. Alternatively, it would be possible to link an iron–sulfur cluster-containing protein directly to a gold electrode by a similar approach with a bivalent tether molecule. These types of experiments are underway and will be reported elsewhere.

Note added in proof

We recently became aware of Brazzolotto et al. J. Biol. Chem. (2006) 281, 769–774 in which an added imidazole was shown by HYSCORE spectroscopy to be the forth ligand to a [4Fe–4S] cluster in the HydF protein of *Thermotoga maritima*.

Acknowledgments

We thank Alan Benesi (director of NMR facility at Pennsylvania State University) for his help and cooperation. Technical help from Andrew Hansen, Bernt Minert and Irina Michin is gratefully acknowledged. We thank Veronica L. Stirewalt for technical assistance in the construction of the site-specific mutations in *psaC*. We are grateful to Keiichi Fukuyama from Department of Biology of the Osaka University for discussions of the structure of mono cluster ferredoxins. We sincerely thank Anton Savitsky for fruitful discussion of magnetic interaction between two reduced iron–sulfur clusters in dicluster ferredoxins. We also thank Dietmar Stehlik for stimulating discussions. We acknowledge Wolfgang Lubitz and Wolfgang Gärtner for use of the biological laboratory at the Max-Planck Institute for Bioinorganic Chemistry, which allowed preparation of the Mössbauer samples of the C13G/C33S PsaC variant. The Max-Planck Society, specifically Max-Planck Institute for Bioinorganic Chemistry, is gratefully acknowledged for funding of the Mössbauer studies. Welch Foundation grant E-1184 to R.S.C. is acknowledged for funding of resonance Raman work. A major portion of the overall work was supported by the Department of Energy (DE-FG-02-98-ER20314) and by the National Science Foundation (MCB-0117079) to J.H.G. the National Science Foundation (MCB-0077586) to D.A.B and Sfb 498 (project A3) to M.L.A. are acknowledged for additional funding.

References

[1] M.D. Toney, J.F. Kirsch, Direct Bronsted analysis of the restoration of activity to a mutant enzyme by exogenous amines, Science 243 (1989) 1485–1488.
[2] D. Duda, C. Tu, M. Qian, P. Laipis, M. Agbandje-McKenna, D.N. Silverman, R. McKenna, Structural and kinetic analysis of the chemical rescue of the proton transfer function of carbonic anhydrase II, Biochemistry 40 (2001) 1741–1748.
[3] P. Adelroth, M.L. Paddock, A. Tehrani, J.T. Beatty, G. Feher, M.Y. Okamura, Identification of the proton pathway in bacterial reaction centers: decrease of proton transfer rate by mutation of surface histidines at H126 and H128 and chemical rescue by imidazole identifies the initial proton donors, Biochemistry 40 (2001) 14538–14546.
[4] H. Matsunami, T. Okajima, S. Hirota, H. Yamaguchi, H. Hori, S. Kuroda, K. Tanizawa, Chemical rescue of a site-specific mutant of bacterial copper amine oxidase for generation of the topa quinone cofactor, Biochemistry 43 (2004) 2178–2187.
[5] S.A. McCartney, E.J. Brignole, K.N. Kolegraff, A.N. Loveland, L.M. Ussin, W. Gibson, Chemical rescue of I-site cleavage in living cells and *in vitro* discriminates between the cytomegalovirus protease, assemblin, and its precursor, pUL80a, J. Biol. Chem. 280 (2005) 33206–33212.
[6] S. Huang, S.C. Tu, Identification and characterization of a catalytic base in bacterial luciferase by chemical rescue of a dark mutant, Biochemistry 37 (1998) 8614.
[7] I.E. Lehoux, B. Mitra, (S)-Mandelate dehydrogenase from *Pseudomonas putida*: mutations of the catalytic base histidine-274 and chemical rescue of activity, Biochemistry 38 (1999) 9948–9955.

[8] Y. Qiao, H. Molina, A. Pandey, J. Zhang, P.A. Cole, Chemical rescue of a mutant enzyme in living cells, Science 311 (2006) 1293–1297.
[9] D.M. Williams, D. Wang, P.A. Cole, Chemical rescue of a mutant protein-tyrosine kinase, J. Biol. Chem. 275 (2000) 38127–38130.
[10] R. Zheng, J.S. Blanchard, Identification of active site residues in *E. coli* ketopantoate reductase by mutagenesis and chemical rescue, Biochemistry 39 (2000) 16244–16251.
[11] M.R. Harpel, F.C. Hartman, Chemical rescue by exogenous amines of a site-directed mutant of ribulose 1,5-bisphosphate carboxylase/oxygenase that lacks a key lysyl residue, Biochemistry 33 (1994) 5553–5561.
[12] W. Jiang, G. Locke, M.R. Harpel, R.A. Copeland, J. Marcinkeviciene, Role of Lys100 in human dihydroorotate dehydrogenase: mutagenesis studies and chemical rescue by external amines, Biochemistry 39 (2000) 7990–7997.
[13] A. Watanabe, Y. Kurokawa, T. Yoshimura, T. Kurihara, K. Soda, N. Esaki, Role of lysine 39 of alanine racemase from *Bacillus stearothermophilus* that binds pyridoxal 5′-phosphate. Chemical rescue studies of Lys39 → Ala mutant, J. Biol. Chem. 274 (1999) 4189–4194.
[14] M. Klimacek, K.L. Kavanagh, D.K. Wilson, B. Nidetzky, On the role of Bronsted catalysis in *Pseudomonas fluorescens* mannitol 2-dehydrogenase, Biochem. J. 375 (2003) 141–149.
[15] S.J. Williams, B.L. Mark, D.J. Vocadlo, M.N. James, S.G. Withers, Aspartate 313 in the *Streptomyces plicatus* hexosaminidase plays a critical role in substrate-assisted catalysis by orienting the 2-acetamido group and stabilizing the transition state, J. Biol. Chem. 277 (2002) 40055–40065.
[16] B. Cobucci-Ponzano, A. Trincone, A. Giordano, M. Rossi, M. Moracci, Identification of the catalytic nucleophile of the family 29 α-L-fucosidase from *Sulfolobus solfataricus via* chemical rescue of an inactive mutant, Biochemistry 42 (2003) 9525–9531.
[17] H. Miyake, C. Otsuka, S. Nishimura, Y. Nitta, Catalytic mechanism of β-amylase from *Bacillus cereus* var. *mycoides*: chemical rescue of hydrolytic activity for a catalytic site mutant (Glu367-(Ala) by azide, J. Biochem. (Tokyo) 131 (2002) 587–591.
[18] D.L. Zechel, S.P. Reid, D. Stoll, O. Nashiru, R.A. Warren, S.G. Withers, Mechanism, mutagenesis, and chemical rescue of a β-mannosidase from *Cellulomonas fimi*, Biochemistry 42 (2003) 7195–7204.
[19] J.L. Viladot, E. de Ramon, O. Durany, A. Planas, Probing the mechanism of *Bacillus* 1,3-1,4-·β-D-glucan 4-glucanohydrolases by chemical rescue of inactive mutants at catalytically essential residues, Biochemistry 37 (1998) 11332–11342.
[20] M. Vallmitjana, M. Ferrer-Navarro, R. Planell, M. Abel, C. Ausin, E. Querol, A. Planas, J.A. Perez-Pons, Mechanism of the family 1 β-glucosidase from *Streptomyces* sp.: catalytic residues and kinetic studies, Biochemistry 40 (2001) 5975–5982.
[21] C.H. Li, S.C. Tu, Probing the functionalities of α-Glu328 and α-Ala74 of *Vibrio harveyi* luciferase by site-directed mutagenesis and chemical rescue, Biochemistry 44 (2005) 13866–13873.
[22] Z. He, M.D. Toney, Direct detection and kinetic analysis of covalent intermediate formation in the 4-amino-4-deoxychorismate synthase catalyzed reaction, Biochemistry 45 (2006) 5019–5028.
[23] T.K. Kim, P. Lee, R.F. Colman, Critical role of Lys212 and Tyr140 in porcine NADP-dependent isocitrate dehydrogenase, J. Biol. Chem. 278 (2003) 49323–49331.
[24] B. Brooks, W.F. Benisek, Specific activation of a tyrosine–glycine mutant of delta 5-3-ketosteroid isomerase by phenols, Biochem. Biophys. Res. Commun. 184 (1992) 1386–1392.
[25] G.H. Lorimer, Y.R. Chen, F.C. Hartman, A role for the epsilon-amino group of lysine-334 of ribulose-1,5-bisphosphate carboxylase in the addition of carbon dioxide to the 2,3-enediol(ate) of ribulose 1,5-bisphosphate, Biochemistry 32 (1993) 9018–9024.
[26] C.E. Hopkins, P.B. O'Connor, K.N. Allen, C.E. Costello, D.R. Tolan, Chemical-modification rescue assessed by mass spectrometry demonstrates that gamma-thia-lysine yields the same activity as lysine in aldolase, Protein Sci. 11 (2002) 1591–1599.
[27] L.M. Gloss, J.F. Kirsch, Examining the structural and chemical flexibility of the active site base, Lys-258, of *Escherichia coli* aspartate aminotransferase by replacement with unnatural amino acids, Biochemistry 34 (1995) 12323–12332.
[28] S. Dementin, A. Bouhss, G. Auger, C. Parquet, D. Mengin-Lecreulx, O. Dideberg, J. van Heijenoort, D. Blanot, Evidence of a functional requirement for a carbamoylated lysine residue in MurD, MurE and MurF synthetases as established by chemical rescue experiments, Eur. J. Biochem. 268 (2001) 5800–5807.
[29] M.A. Pearson, R.A. Schaller, L.O. Michel, P.A. Karplus, R.P. Hausinger, Chemical rescue of *Klebsiella aerogenes* urease variants lacking the carbamylated-lysine nickel ligand, Biochemistry 37 (1998) 6214–6220.
[30] W. Fu, S. Ohandley, R. Cunningham, M. Johnson, The role of the iron–sulfur cluster in *Escherichia coli* endonuclease-III—A resonance Raman study, J. Biol. Chem. 267 (1992) 16135–16137.
[31] M.H. Emptage, T.A. Kent, M.C. Kennedy, H. Beinert, E. Munck, Mössbauer and EPR studies of activated aconitase: development of a localized valence state at a subsite of the [4Fe–4S] cluster on binding of citrate, Proc. Natl. Acad. Sci. U. S. A. 80 (1983) 4674–4678.
[32] H. Beinert, M.C. Kennedy, Aconitase, a 2-faced protein—Enzyme and iron regulatory factor, FASEB J. 7 (1993) 1442–1449.
[33] H. Beinert, P.J. Kiley, Fe–S proteins in sensing and regulatory functions, Curr. Opin. Chem. Biol. 3 (1999) 152–157.
[34] J.T. Jarrett, The novel structure and chemistry of iron–sulfur clusters in the adenosylmethionine-dependent radical enzyme biotin synthase, Arch. Biochem. Biophys. 433 (2005) 312–321.
[35] G. Shen, J.H. Golbeck, Assembly of the bound iron–sulfur clusters in Photosystem I, in: J. Golbeck (Ed.), Photosystem I: The Light-Driven Plastocyanin:Ferredoxin Oxidoreductase, Springer, Dordrecht, 2006, pp. 529–547.
[36] R.D. Britt, K. Sauer, M.P. Klein, D.B. Knaff, A. Kriauciunas, C.-A. Yu, L. Yu, R. Malkin, Electron spin echo envelope modulation spectroscopy supports the suggested coordination of two histidine ligands to the Rieske Fe–S centers of the cytochrome b_6f complex of spinach and the cytochrome bc_1 Complexes of *Rhodospirillum rubrum, Rhodobacter sphaeroides* R26, and bovine heart mitochondria, Biochemistry 30 (1991) 1892–1901.
[37] J. Zhao, N. Li, P. Warren, J.H. Golbeck, D. Bryant, Site-directed conversion of a cysteine to aspartate leads to the assembly of a [3Fe–4S] cluster in PsaC of Photosystem I—The photoreduction of F_A is independent of F_B, Biochemistry 31 (1992) 5093–5099.
[38] T. Mehari, F.Y. Qiao, M.P. Scott, D.F. Nellis, J.D. Zhao, D.A. Bryant, J.H. Golbeck, Modified ligands to F_A and F_B in Photosystem I. 1. Structural constraints for the formation of iron–sulfur clusters in free and rebound PsaC, J. Biol. Chem. 270 (1995) 28108–28117.
[39] L. Yu, D.A. Bryant, J.H. Golbeck, Evidence for a mixed-ligand [4Fe–4S] cluster in the C14D mutant of PsaC. Altered reduction potentials and EPR spectral properties of the F_A and F_B clusters on rebinding to the P700-F_X core, Biochemistry 34 (1995) 7861–7868.
[40] L.A. Yu, I.R. Vassiliev, Y.S. Jung, D.A. Bryant, J.H. Golbeck, Modified ligands to F_A and F_B in Photosystem I. 2. Characterization of a mixed ligand [4Fe–4S] cluster in the C51D mutant of PsaC upon rebinding to P700-FX cores, J. Biol. Chem. 270 (1995) 28118–28125.
[41] Y.S. Jung, I.R. Vassiliev, F.Y. Qiao, F. Yang, D.A. Bryant, J.H. Golbeck, Modified ligands to F_A and F_B in Photosystem I—Proposed chemical rescue of a [4Fe–4S] cluster with an external thiolate in alanine, glycine, and serine mutants of PsaC, J. Biol. Chem. 271 (1996) 31135–31144.
[42] J.H. Golbeck, Photosystem I in cyanobacteria, in: D.A. Bryant (Ed.), The Molecular Biology of Cyanobacteria, Kluwer Academic Publishers, The Netherlands, 1994, pp. 179–220.
[43] M.L. Antonkine, G.H. Liu, D. Bentrop, D.A. Bryant, I. Bertini, C. Luchinat, J.H. Golbeck, D. Stehlik, Solution structure of the unbound, oxidized Photosystem I subunit PsaC, containing 4Fe–4S clusters F_A and F_B: a conformational change occurs upon binding to Photosystem I, J. Biol. Inorg. Chem. 7 (2002) 461–472.
[44] P. Jordan, P. Fromme, H.T. Witt, O. Klukas, W. Saenger, N. Krauss, Three-dimensional structure of cyanobacterial photosystem I at 2.5 Å resolution, Nature 411 (2001) 909–917.
[45] M.L. Antonkine, P. Jordan, P. Fromme, N. Krauss, J.H. Golbeck, D. Stehlik, Assembly of protein subunits within the stromal ridge of Photosystem I. Structural changes between unbound and sequentially

PS I-bound polypeptides and correlated changes of the magnetic properties of the terminal iron sulfur clusters, J. Mol. Biol. 327 (2003) 671–697.
[46] J.H. Golbeck, A comparative analysis of the spin state distribution of *in vivo* and *in vitro* mutants of PsaC. A biochemical argument for the sequence of electron transfer in Photosystem I as $F_X \rightarrow F_A \rightarrow F_B \rightarrow$ ferredoxin/flavodoxin, Photosynth. Res. 61 (1999) 107–149.
[47] L. Yu, J.D. Zhao, W.P. Lu, D.A. Bryant, J.H. Golbeck, Characterization of the [3Fe–4S] and [4Fe–4S] clusters in unbound PsaC mutants C14D and C51D—Midpoint potentials of the single [4Fe–4S] clusters are identical to F_A and F_B in bound PsaC of Photosystem I, Biochemistry 32 (1993) 8251–8258.
[48] W. Lovenberg, B.B. Buchanan, J.C. Rabinowitz, Studies on the chemical nature of clostridial ferredoxin, J. Biol. Chem. 238 (1963) 3899–3913.
[49] F. Bonomi, M.T. Werth, D.M. Kurtz Jr., Assembly of $[Fe_2S_2(Sr)_4]^{2-}$, $[Fe_4S_4(Sr)_4]^{2-}$ in aqueous-media from iron salts, thiols, and sulfur, sulfide, or thiosulfate plus rhodanese, Inorg. Chem. 24 (1985) 4331–4335.
[50] M.A. Bobrik, L. Que Jr., R.H. Holm, Synthetic analogs of the active sites of iron–sulfur proteins: IV. Ligand substitution reactions of the tetranuclear clusters $(Fe_4S_4(Sr)_4)^2$, J. Am. Chem. Soc. 96 (1974) 285–287.
[51] J. Zhao, P.V. Warren, N. Li, D.A. Bryant, J.H. Golbeck, Reconstitution of electron transport in Photosystem I with PsaC and PsaD proteins expressed in *Escherichia coli*, FEBS Lett. 276 (1990) 175–180.
[52] M.L. Antonkine, D. Bentrop, I. Bertini, C. Luchinat, G. Shen, D.A. Bryant, D. Stehlik, J.H. Golbeck, Paramagnetic ^{1}H NMR spectroscopy of the reduced, unbound Photosystem I subunit PsaC: sequence-specific assignment of contact-shifted resonances and identification of mixed- and equal-valence Fe–Fe pairs in [4Fe–4S] centers F_A^- and F_B^-, J. Biol. Inorg. Chem. 5 (2000) 381–392.
[53] F. Yang. PhD thesis in Chemistry, pp. 204, University of Nebraska-Lincoln, Lincoln NE, USA, 1998.
[54] G.L. Ellman, Tissue sulfhydryl groups, Arch. Biochem. Biohys. 82 (1959) 70–77.
[55] G. Bulaj, T. Kortemme, D.P. Goldenberg, Ionization–reactivity relationships for cysteine thiols in polypeptides, Biochemistry 37 (1998) 8965–8972.
[56] M.C. Kennedy, T.A. Kent, M. Emptage, H. Merkle, H. Beinert, E. Munck, Evidence for the formation of a linear [3Fe–4S] cluster in partially unfolded aconitase, J. Biol. Chem. 259 (1984) 14463–14471.
[57] J.H. Golbeck, S. Lien, A. San Pietro, Quantitation of labile sulfide content and P700 photochemistry in spinach Photosystem I particles, Biochem. Biophys. Res. Commun. 71 (1976) 452–458.
[58] R.S. Czernuszewicz, Resonance Raman spectroscopy of metalloproteins using CW excitation, in: C. Jones, B. Mulloy, A.H. Thomas (Eds.), Spectroscopic Methods and Analyses, Humana Press Inc., 999 Riverview Dr, Suite 208, Totowa, NJ 07512, 1993, pp. 345–374.
[59] R.S. Czernuszewicz, M.K. Johnson, A simple low-temperature cryostat for resonance Raman studies of frozen protein solutions, Appl. Spectrosc. 37 (1983) 297–298.
[60] T.G. Spiro, R.S. Czernuszewicz, S. Han, Iron–sulfur proteins and analog complexes, in: T.G. Spiro (Ed.), Biological Applications of Raman Spectroscopy, Wiley-Interscience, New York, 1998, pp. 523–553.
[61] R.S. Czernuszewicz, K.A. Macor, M.K. Johnson, A. Gewirth, T.G. Spiro, Vibrational-mode structure and symmetry in proteins and analogs containing Fe_4S_4 clusters—Resonance Raman evidence for different degrees of distortion in HiPIP and ferredoxin, J. Am. Chem. Soc. 109 (1987) 7178–7187.
[62] E.C. Duin, M.E. Lafferty, B.R. Crouse, R.M. Allen, I. Sanyal, D.H. Flint, M.K. Johnson, [2Fe–2S] to [4Fe–4S] cluster conversion in *Escherichia coli* biotin synthase, Biochemistry 36 (1997) 11811–11820.
[63] M.K. Johnson, R.S. Czernuszewicz, T.G. Spiro, J.A. Fee, W.V. Sweeney, Resonance Raman-spectroscopic evidence for a common [3Fe–4S] structure among proteins containing 3-Iron centers, J. Am. Chem. Soc. 105 (1983) 6671–6678.
[64] P.R. Conover, A.T. Kowal, W. Fu, J.-B. Park, S. Aono, M.W.W. Adams, M.K. Johnson, Spectroscopic characterization of the novel iron–sulfur cluster in *Pyrococcus furiosus* ferredoxin, J. Biol. Chem. 265 (1990) 8533–8541.
[65] P. Middleton, D.P.E. Dickson, C.E. Johnson, J.D. Rush, Interpretation of Mössbauer-spectra of 4-Iron ferredoxin from *Bacillus stearothermophilus*, Eur. J. Biochem. 88 (1978) 135–141.
[66] V. Schuenemann, H. Winker, Structure and dynamics of biomolecules studied by Mössbauer spectroscopy, Rep. Prog. Phys. 63 (2000) 263–353.
[67] A.H. Robbins, C.D. Stout, Structure of activated aconitase: formation of the [4Fe–4S] cluster in the crystal, Proc. Natl. Acad. Sci. U. S. A. 86 (1989) 3639–3643.
[68] P.K. Mascharak, M.C. Smith, W.H. Armstrong, B.K. Burgess, R.H. Holm, Fluorine-19 chemical shifts as structural probes of metal–sulfur clusters and the cofactor of nitrogenase, Proc. Natl. Acad. Sci. U. S. A. 79 (1982) 7056–7060.
[69] G.B. Wong, D.M.J. Kurtz, R.H. Holm, L.E. Mortenson, R.G. Upchurch, A ^{19}F NMR method for identification of iron–sulfur cores extruded from active centers of proteins, with applications to milk xanthine oxidase and the iron–molybdenum proteins of nitrogenase, J. Am. Chem. Soc. 101 (1979) 3078–3090.
[70] D.M. Kurtz, G.B. Wong, R.H. Holm, Structural identification of the extruded cores of the active centers of iron–sulfur proteins by fluorine-19 nuclear magnetic resonance spectroscopy. Application to milk xanthine oxidase. J. Am. Chem. Soc. 100 (1978) 6777–6779.
[71] P.K. Mascharak, M.C. Smith, W.H. Armstrong, B.K. Burgess, R.H. Holm, Fluorine-19 chemical shifts as structural probes of metal–sulfur clusters and the cofactor of nitrogenase, Proc. Natl. Acad. Sci. U. S. A. 79 (1982) 7056–7060.
[72] R.C. Conover, A.T. Kowal, W.G. Fu, J.B. Park, S. Aono, M.W. Adams, M.K. Johnson, Spectroscopic characterization of the novel iron–sulfur cluster in *Pyrococcus furiosus* ferredoxin, J. Biol. Chem. 265 (1990) 8533–8541.
[73] S.J. George, F.A. Armstrong, E.C. Hatchikian, A.J. Thomson, Electrochemical and spectroscopic characterization of the conversion of the 7Fe into the 8Fe form of ferredoxin III from *Desulfovibrio africanus*. Identification of a [4Fe–4S] cluster with one non-cysteine ligand, Biochem. J. 264 (1989) 275–284.
[74] P.A. Lindahl, E.P. Day, T.A. Kent, W.H. Orme-Johnson, E. Munck, Mössbauer, EPR, and magnetization studies of the *Azotobacter vinelandii* Fe protein. Evidence for a $[4Fe–4S]^{1+}$ cluster with spin S = 3/2, J. Biol. Chem. 260 (1985) 11160–11173.
[75] M.J. Carney, G.C. Papaefthymiou, R.B. Frankel, R.H. Holm, Alternative spin states in synthetic analogues of biological $[4Fe–4S]^+$ clusters: further cases of variable ground states and the structure of $(Et_4N)_3[Fe_4S_4(S–O–C6H_4StBu)^4]$, containing a reduced cluster with a compressed tetragonal distortion, J. Am. Chem. Soc. 28 (1989) 1497–1503.
[76] K. Fukuyama, T. Okada, Y. Kakuta, Y. Takahashi, Atomic resolution structures of oxidized 4Fe–4S ferredoxin from *Bacillus thermoproteolyticus* in two crystal forms: systematic distortion of 4Fe–4S cluster in the protein, J. Mol. Biol. 315 (2002) 1155–1166.
[77] M.J. Carney, G.C. Papaefthymiou, K. Spartalians, R.B. Frankel, R.H. Holm, Ground Spin state variability in $[Fe_4S_4(Sr)_4]^{3-}$-synthetic analogs of the reduced clusters in ferredoxins and other iron sulfur proteins—Cases of extreme sensitivity of electronic state and structure to extrinsic factors, J. Am. Chem. Soc. 110 (1988) 6084–6095.
[78] J.N. Butt, A. Sucheta, F.A. Armstrong, J. Breton, A.J. Thomson, E.C. Hatchikian, Voltammetric characterization of rapid and reversible binding of an exogenous thiolate ligand at a [4Fe–4S] cluster in ferredoxin-III from *Desulfovibrio africanus*, J. Am. Chem. Soc. 115 (1993) 1413–1421.
[79] J.L.H. Busch, J.L. Breton, B.M. Bartlett, F.A. Armstrong, R. James, A.J. Thomson, [3Fe–4S] ↔ [4Fe–4S] cluster interconversion in *Desulfovibrio africanus* ferredoxin III: properties of an Asp(14) → Cys mutant, Biochem. J. 323 (1997) 95–102.
[80] S.E. Mulholland, B.R. Gibney, F. Rabanal, P.L. Dutton, Characterization of the fundamental protein ligand requirements of $[4Fe–4S]^{2+/+}$ clusters with

sixteen amino acid maquettes, J. Am. Chem. Soc. 120 (1998) 10296–10302.
[81] B.R. Gibney, S.E. Mulholland, F. Rabanal, P.L. Dutton, Ferredoxin and ferredoxin-heme maquettes, Proc. Natl. Acad. Sci. U. S. A. 93 (1996) 15041–15046.
[82] B. Shen, D.R. Jollie, T.C. Diller, C.D. Stout, P.J. Stephens, B.K. Burgess, Site-directed mutagenesis of *Azotobacter vinelandii* ferredoxin I: cysteine ligation of the [4Fe–4S] cluster with protein rearrangement is preferred over serine ligation, Proc. Natl. Acad. Sci. U. S. A. 92 (1995) 10064–10068.
[83] J.G. Huber, J. Gaillard, J.M. Moulis, NMR of *Chromatium vinosum* ferredoxin: evidence for structural inequivalence and impeded electron transfer between the two [4Fe–4S] clusters, Biochemistry 34 (1995) 194–205.
[84] P. Kyritsis, R. Kummerle, J.G. Huber, J. Gaillard, B. Guigliarelli, C. Popescu, E. Munck, J.M. Moulis, Unusual NMR, EPR, and Mössbauer properties of *Chromatium vinosum* 2[4Fe–4S] ferredoxin, Biochemistry 38 (1999) 6335–6345.
[85] L. Calzolai, C.M. Gorst, K.L. Bren, Z.H. Zhou, M.W.W. Adams, G.N. LaMar, Solution NMR study of the electronic structure and magnetic properties of cluster ligation mutants of the four-iron ferredoxin from the hyperthermophilic archaeon *Pyrococcus furiosus*, J. Am. Chem. Soc. 119 (1997) 9341–9350.